Dynamic Analysis of the Doubly Fed Induction Generator Connected to Power System under Wind Speed Fluctuation

Hung-Cheng Chen Tien- Ting Chang Jhong- Sian Jian
Department of Electrical Engineering
National Chin-Yi University of Technology
Taichung, TAIWAN.
hcchen@ncut.edu.tw ctt@ncut.edu.tw ewq428@yahoo.com.tw

Abstract

The wind is the driving force for wind turbine, and it directly determines the dynamic characteristics of generator. Due to its randomness and intermittence, wind energy has great effect on the quality and security of operation of power system. The main emphasis of this paper is to study the effect of wind speed fluctuation on the doubly fed induction generator connected to power system. Firstly, the mathematical models of a 3.6MW doubly fed induction generator and different wind patterns are derived. The MATLAB/Simulink software is then used to model the wind, wind turbine, doubly fed induction generator, and its controllers. Simulation results obtained from the model are used to analyze the effects of different wind speed fluctuation on system dynamic responses.

Keywords: wind turbine, MATLAB/Simulink, Doubly fed induction generator

1. Introduction

The wind power is a kind of renewable green power sources. It is a permanent source with no exploring and transporting. To solve the problem of energy's shortage and improve the environment quality, wind power is used to produce electricity by a lot of countries. The power output of a wind power plant is stochastic, which is determined by the wind and wind turbine generators. If a wind plant has more wind turbine generators, the change of its power output will become drastic. With the development of wind industry, this kind of large wind plants will bring many problems to the power system's operating. Due to the quick development of power electronics and relative applications at present, the variable speed wind turbine with doubly fed induction generator (DFIG) was turned into mainstream machine in the field of exploiting wind energy in the world now. Compared to wind turbines using fixed speed induction generators, DFIG-based wind turbines offer several advantages including four-quadrant active and reactive power capabilities, and variable speed operation. Such system also results in lower converter costs and lower power losses compared to a system based on a fully fed synchronous generator with full-rated converter. Therefore, the variable-speed constant-frequency (VSCF) doubly fed wind turbine technology and operational characteristics should be an important field of wind energy research. In this paper, we study the character of the wind power system and build the mathematical models accordingly. The MATLAB/Simulink models of a complete 3.6MW DFIG generation system and three different types of wind, including fitful wind, gradation wind, and random wind, are also built. Based on these models, the effects of wind speed fluctuation on the operation characteristics of DFIG connected to power system are studied by dynamic simulation. From the analysis of the simulation results, we can realize that the wind plant's power output will keep varying with the change of the wind speed.

2. STRUCTURE OF SYSTEM

2.1 The mathematical model of DFIG

To assume a DFIG in a d-q reference frame rotating at synchronous angular speed, neglected the stator and rotor variables. The classical electrical equations of the DFIG are written as follows [5]、[6]

$$\begin{aligned} v_{ds} &= -i_{ds}R_s + \frac{d\psi_{ds}}{dt} - \omega_1\psi_{qs} \\ v_{qs} &= -i_{qs}R_s + \frac{d\psi_{qs}}{dt} + \omega_1\psi_{ds} \\ v_{dr} &= i_{dr}R_r + \frac{d\psi_{dr}}{dt} - \omega_s\psi_{qr} \\ v_{qr} &= i_{qr}R_r + \frac{d\psi_{qr}}{dt} + \omega_s\psi_{dr} \end{aligned} \quad (1)$$

The flux equations are

$$\begin{aligned} \psi_{ds} &= -L_s i_{ds} + L_m i_{dr} \\ \psi_{qs} &= -L_s i_{qs} + L_m i_{qr} \\ \psi_{dr} &= -L_r i_{dr} + L_m i_{ds} \\ \psi_{qr} &= -L_r i_{qr} + L_m i_{ds} \end{aligned} \quad (2)$$

Where ω_1 ：synchronous angular frequency

ω_s ：slip angular frequency

R_s 、R_r ：stator and rotor winding equivalent resistance

L_s 、L_r 、L_m ：stator and rotor winding self inductance and mutual inductance

The motion equations are given as follows:

$$\frac{d\omega_r}{dt} = (T_m - T_e)/J$$

$$T_e = \frac{3}{2} N_p L_m (i_{qs} i_{dr} - i_{ds} i_{qr}) \quad (3)$$

$$\omega_s = s\omega_1 = \omega_1 - \omega_r$$

$$\frac{d\delta}{dt} = \omega_r$$

where ω_r ：rotor angular frequency

s ： slip

T_m ：mechanical torque provided for the wind turbine

T_e ：electromagnetic torque

J ：moment of inertia

2.2 Mathematical model of the grid-side Converter

Grid-side converter is a simply AC / DC converter. It could work in the rectifier state and the inverter state. That is the major implementation elements of the DFIG slip power flow control. So we established the mathematical model of PWM rectifier to study the three-phase PWM converter operation control.

AC equivalent diagram of the supply side converter is as shown in Figure1.

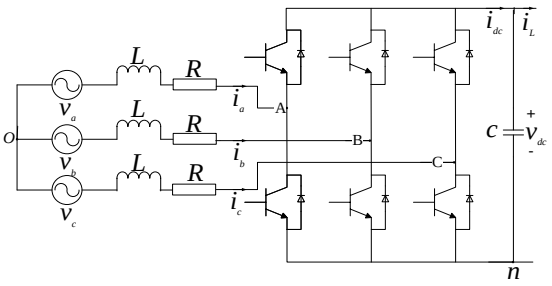

Fig. 1 Grid-side converter arrangement.

The voltage balance across the inductors is

$$C\frac{d}{dt}v_{dc} = i_{dc} - i_L = S_a \cdot i_a + S_b \cdot i_b + S_c \cdot i_c - i_L \quad (4)$$

$$\begin{bmatrix} v_a \\ v_b \\ v_c \end{bmatrix} = R\begin{bmatrix} i_a \\ i_b \\ i_c \end{bmatrix} + L\frac{d}{dt}\begin{bmatrix} i_a \\ i_b \\ i_c \end{bmatrix} + \begin{bmatrix} S_a \\ S_b \\ S_c \end{bmatrix} v_{dc} + \begin{bmatrix} u_n \\ u_n \\ u_n \end{bmatrix} \quad (5)$$

Where S_a 、S_b 、S_c represented three-phase bridge arm switching function, respectively.

S =1 means the top switch is on and bottom is close

S =0 means the bottom switch is on and top is close

i_{dc} = DC-link output current

i_L = DC-link load current

v_{dc} = DC-link output voltage

C = filter capacitor

L = inductance of grid-side reactor

R = resistance of grid-side reactor

Due to the total amount of the three-phase currents of non-midline system is zero

i.e., $i_a + i_b + i_c = 0$ can obtain

$$u_n = \frac{v_a + v_b + v_c}{3} - \frac{1}{3}(S_a + S_b + S_c)v_{dc} \quad (6)$$

To utilize coordinate transformation and defined i_d, i_q and v_{dc} be state variables. Therefore, there-phase converter can be a mathematical model of two-phase rotating coordinate.

$$u_d = -L\frac{d}{dt}i_d - Ri_d + \omega_1 L i_q + v_d$$

$$u_q = -L\frac{d}{dt}i_q - Ri_q - \omega_1 L i_d + v_q \quad (7)$$

$$C\frac{d}{dt}v_{dc} = i_{dc} - i_L$$

Where u_d 、u_q ：the d-q components of bridge arm output voltage

v_d 、v_q ：the d-q components of grid voltage

i_d 、i_q ：the d-q components of input currents

Under the synchronously rotating frame, the d axis aligned with the grid voltage vector position. The grid voltage components are

$$v_d = const$$

$$v_q = 0 \quad (8)$$

Neglecting the harmonics due to switching in the converter and the machine losses or converter losses. The active power balance equation is as follows:

$$P_r = v_{dc} i_{dc} = \frac{3}{2}(v_d i_d + v_q i_q) = \frac{3}{2} v_d i_d \quad (9)$$

While $P_r > 0$, it represents grid-side converter work in the rectifier state and absorb energy from the grid. While $P_r < 0$, it represents grid-side converter work in the inverter state and energy back to the grid from the DC-side.

With the PWM depth, m_1, as known,

$$v_d = \frac{m_1}{2\sqrt{2}} v_{dc} \quad (10)$$

From equation(9)

$$i_{dc} = \frac{3 m_1 i_d}{4\sqrt{2}} \quad (11)$$

The DC link voltage link equation is

$$C\frac{dv_{dc}}{dt} = i_{dc} - i_L = \frac{3 m_1 i_d}{4\sqrt{2}} - i_L \quad (12)$$

It is evident from equation(12) that DC link voltage v_{dc} may be controlled through i_d control. The reactive power from (to) the source Q_r is

$$Q_r = \frac{3}{2}(v_d i_q - v_q i_d) = \frac{3}{2} v_d i_q \quad (13)$$

We can know from the above equations that the reactive power to the grid-side converter from the source or to the source from the grid-side converter that can be controlled through i_q. If the grid-side be controlled with a unit power factor, the i_q command value is equal to 0. The assumptions are as

$$u_{d1} = Ri_d + L\frac{d}{dt}i_d$$
$$u_{q1} = Ri_q + L\frac{d}{dt}i_q \quad (14)$$

Through the compensate terms to u_d and u_q. To eliminate the effect of the cross-coupling to the input AC current. Simultaneously to join the feedforward compensation of the grid voltage. We can obtain the reference voltage u_d^* and u_q^*

$$u_d^* = -u_{d1} + (\omega_e L i_q + v_d)$$
$$u_q^* = -u_{q1} - (\omega_e L i_d) \quad (15)$$

The grid-side converter vector control model can be obtained from the above analysis. It was be shown in Figure.2

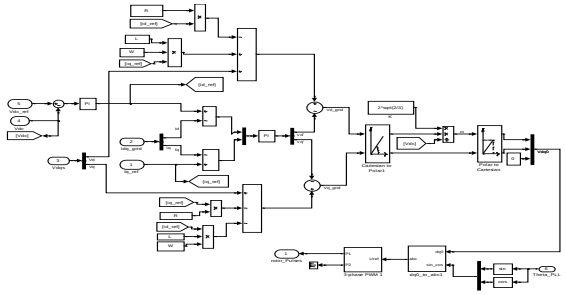

Fig. 2 Modeling of the grid-side converter

2.3 Mathematical model of the rotor-side converter

Neglect the resistance of the generator stator winding. The stator flux and the stator voltage vector phase just right difference of 90°. Therefore, to utilize the stator flux-oriented to the d axis aligned with the stator flux vector position. The flux equation is

$$\psi_{ds} = \psi_s$$
$$\psi_{qs} = 0 \quad (16)$$

To keep the stator flux ψ_s as a constant, the voltage equations can be expressed as

$$v_{ds} \approx \frac{d}{dt}\psi_s = 0$$
$$v_{qs} \approx \omega_1 \psi_s = V_s \quad (17)$$

Where V_s is stator voltage space vector

The active and reactive stator powers P_s, Q_s are as follows:

$$P = \frac{3}{2}(v_{ds}i_{ds} + v_{qs}i_{qs}) \approx \frac{3}{2}V_s i_{qs}$$
$$Q = \frac{3}{2}(v_{qs}i_{ds} - v_{ds}i_{qs}) \approx \frac{3}{2}V_s i_{ds} \quad (18)$$

Based on (18), While DFIG connected to infinite grid, it can be deem that the stator voltage is constant. Only the stator current is the controlled quantity. Therefore, controlled of the DFIG output power connected to power systems which can be to the stator current control. Achieves the goal of the DFIG output active and reactive can be controlled, respectively.

As the stator windings directly connected to the power systems, and the effect of the stator resistance is very small. It can be considered that the equivalent stator magnetizing current as a constant, i.e.

$$i_{ms} = \frac{\psi_s}{L_m} \approx \frac{V_s}{L_m \omega_1} \quad (19)$$

According to (2), d-q axis stator current can be calculated as

$$i_{ds} = \frac{L_m i_{dr} - \psi_{ds}}{L_s} = \frac{L_m(i_{dr} - i_{ms})}{L_s}$$
$$i_{qs} = \frac{L_m}{L_s} i_{qr} \quad (20)$$

Substituting (20) into (1), the rotor voltage can be express as

$$v_{dr} = i_{dr}R_r + \sigma L_r \frac{d}{dt}i_{dr} - \omega_s \sigma L_r i_{qr}$$
$$v_{qr} = i_{qr}R_r + \sigma L_r \frac{d}{dt}i_{qr} + \omega_s(\sigma L_r i_{dr} + \frac{L_m^2}{L_s}i_{ms}) \quad (21)$$

where $\sigma = 1 - \frac{L_m^2}{L_s L_r}$ is the leakage factor

The control variables v_{dr}、v_{qr} of the rotor voltage can be obtained from (21). The cross-coupling produces little influence between the rotor current d-q axis component. May eliminate the cross-coupling influence adopt the control law, and the model of the rotor-side converter vector control is shown in Fig.3

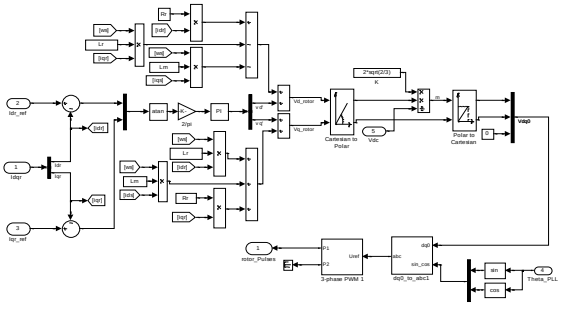

Fig. 3 Modeling of the rotor-side converter

The mathematical models of a 3.6MW doubly fed induction generator and different wind patterns are derived. The MATLAB/Simulink software is then used to model the wind, wind turbine, doubly fed induction generator, and its controllers. The model of DFIG-based wind generation is shown in Fig. 4. This system consists of a doubly fed induction generator with a four-quadrant ac-to-ac converter based on IGBTs connected to the rotor winding, and the stator winding directly connects to power systems. The rotor of the wind turbine is coupled to the generator shaft with a gear box.

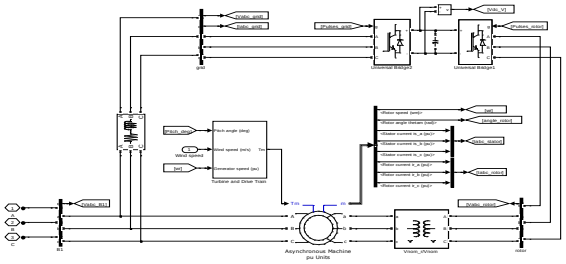

Fig. 4 Model of DFIG-based wind generation

2.4 The dynamic model of a 3.6MW DFIG connected to power systems

The simulation structure of a DFIG-based wind generation and grid connection is shown in Fig. 5. The output voltage of doubly fed induction generator is 4160V, which is increased to 22.8kV by a step-up transformer and connected to a power system through a 20km transmission line. The power system's rating voltage is 161kV which is dropped to 22.8kV by a step-down transformer. Based on these models, the effects of wind speed fluctuation on the operation characteristics of DFIG connected to power system are studied by dynamic simulation.

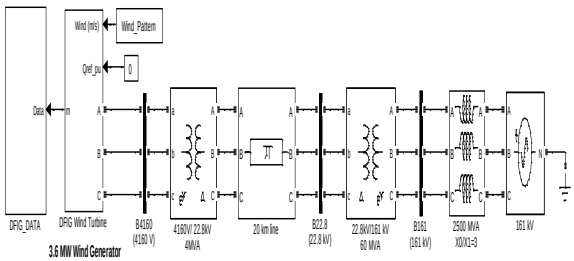

Fig. 5 Simulation structure of the DFIG-base wind generation and grid connection

3. Wind modeling

We utilized mathematical formulas to describe the variation of the wind speed, and built the three wind pattern models which are detailed described in the following.

3.1 Fitful wind

To utilize mathematical formulas to establish the model of the fitful wind. The basic wind velocity is 15m/s. Simulating the begin rise time of the wind is at 5s. The fitful wind continuous for 6s and the intensity is 2m/s as shown in Fig.6.

$$v_{WG} = \begin{cases} 0, & t < t_{1G} \\ v_{COS}, & t_{1G} < t < t_{1G} + t_G \\ 0, & t > t_{1G} + t_G \end{cases} \qquad (22)$$

$$v_{COS} = \frac{MaxG}{2}\left[1 - \cos 2\left(\frac{t}{t_G} - \frac{t_{1G}}{t_G}\right)\pi\right]$$

Where t_{1G} : start-up time (s) ,

t_G : variation cycle (s)

$MaxG$: the maximum fitful wind (m/s)

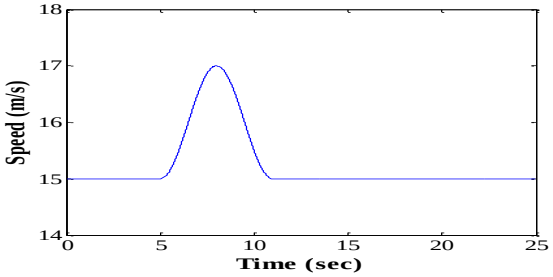

Fig. 6 Simulation of fitful wind

3.2 Gradation wind

To utilize mathematical formulas to establish the model of the gradation wind. The basic wind velocity is 12m/s. Simulating produces a gradation wind at 5s. The strong wind continuous for 5s and the intensity is 4m/s as shown in Fig.7

.

$$v_{WR} = \begin{cases} 0 & (t < t_{1R}) \\ v_{ramp}(t_{1R} \le t < t_{2R}) \\ MaxR(t_{2R} \le t < t_{2R} + t_R) \\ 0 & (t \ge t_{2R} + t_R) \end{cases} \qquad (23)$$

$$v_{ramp} = MaxR\left(1 - \frac{t - t_{2R}}{t_{1R} - t_{2R}}\right)$$

where t_{1R} : increment of the start time (s)

t_{2R} : increment of the cut-off time (s)

t_R : increment of the stop time (s)

$MaxR$: the maximum gradation wind (m/s)

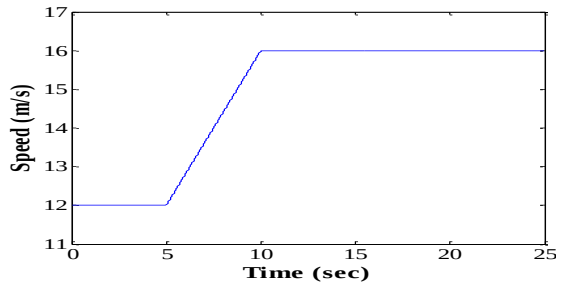

Fig. 7 Simulation of gradation wind

3.3 Random wind

To utilize mathematical formulas to establish the model of the random wind. The basic wind velocity is 15m/s as shown in Fig.8.

$$v_{WN} = v_N Ran(-1,1)\cos(\omega_v t + \phi_v) \qquad (24)$$

Where v_N : base value of random wind (m/s)

$Ran(-1,1)$: random sampling value (range between -1 to 1)

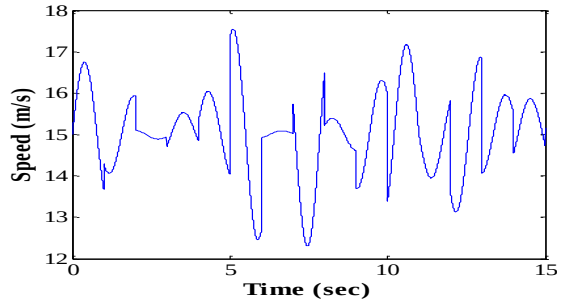

Fig. 8 Simulation of random wind

4. Simulation Results

4.1 Dynamic simulation of the DFIG under a fitful wind action

The dynamic responses of the DFIG generation system under a fitful wind action are shown in Fig. 9. The output active power of the DFIG increases to 3.85MW at 8s while the wind speed arrives at maximum wind speed 17 m/s at the same time as shown in Fig. 9(a). Due to the temporary wind speed variation, the rotor speed shown in Fig. 9(c) reduces after increasing and goes back to original speed 1.2pu because of the pitch angle of wind turbine adjusted accordingly. The variation of the active power output is therefore temporary and settles down at the original power output 3.6MW. The controlled pitch angle of wind turbine to maintain constant power is shown in Fig. 9(d). The pitch angle adjustment results in wind energy conversion under the maximum security. In Fig. 9(b) the variation of the reactive power output followed the wind speed fluctuation is pretty small. The zero-reactive-power control in the ac-to-ac converter keeps the reactive power output near zero regardless of the wind speed fluctuation. The voltages at bus B4160 and B22.8 shown in Fig. 9(e) and 9(g) maintain at 1pu. The currents at bus B4160 and B22.8 shown in Fig. 9(f) and 9(h) vary with the wind speed fluctuation. The DC link voltage also varies with the wind speed fluctuation, but the variation is not obvious as shown in Fig. 9(i). While the wind stops change all of the output variables eventually revert to original values.

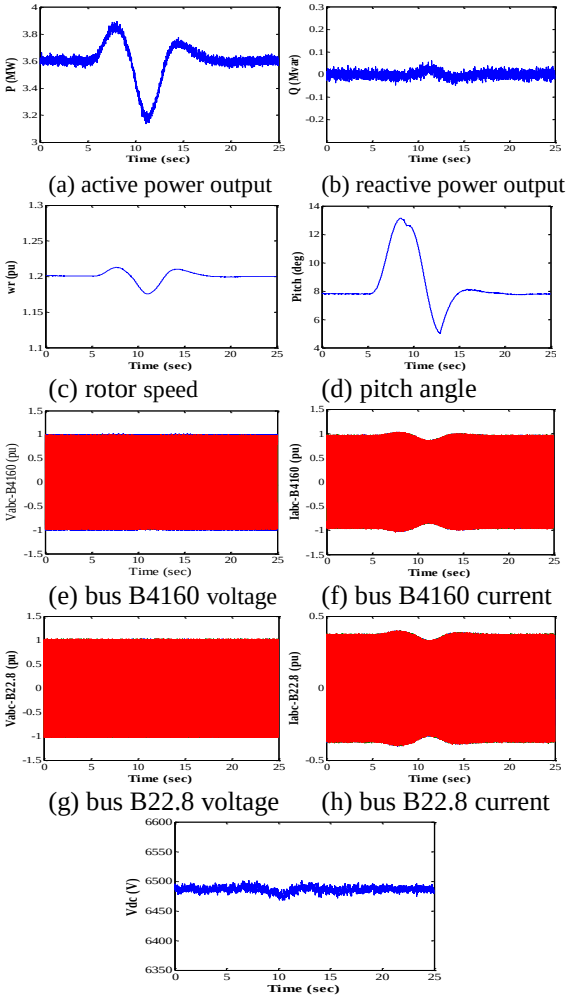

(a) active power output (b) reactive power output

(c) rotor speed (d) pitch angle

(e) bus B4160 voltage (f) bus B4160 current

(g) bus B22.8 voltage (h) bus B22.8 current

(i) dc-link voltage

Fig. 9 Dynamic responses of the DFIG under the fitful wind action

4.2 Dynamic simulation of the DFIG under a gradation wind action

The speed variation of the gradation wind studies here is to linearly increase from 12m/s to 16m/s in 5 seconds. The dynamic responses of the DFIG generation system under the gradation wind action are shown in Fig. 10. The original wind speed and active power output are 12m/s and 3.05MW, respectively. While the wind speed increases to 16m/s at 10s, the active power consequently increases to 3.95MW and then goes back to 3.6MW because of the pitch angle adjustment as shown in Fig. 10(d).

The pitch angle approaches to 0 degree when the wind speed is below the rated wind speed (14m/s) of the DFIG to take advantage the wind energy by the optimal windward angle and generate the maximum output power. When the wind speed arrives to 16m/s, the pitch angle is adjusted to 10.5 degrees to keep the output power at rating and avoid an overload. The rotor speed also varies with the wind speed fluctuation. Although the wind speed has changed from 12m/s to 16m/s, the rotor speed shown in Fig. 10(c) reduces after increasing and goes back to original speed 1.2pu because of the pitch angle control. The reactive power output is shown in Fig. 10(b). The zero-reactive-power control in the ac-to-ac converter keeps the reactive power output near zero regardless of the wind speed fluctuation. The voltages at bus B4160 and B22.8 shown in Fig. 10(e) and 10(g) maintain at 1pu. The currents at bus B4160 and B22.8 shown in Fig. 10(f) and 10(h) vary with the wind speed fluctuation. The DC link voltage varies with the wind speed fluctuation, but the variation is not obvious as shown in Fig. 10(i).

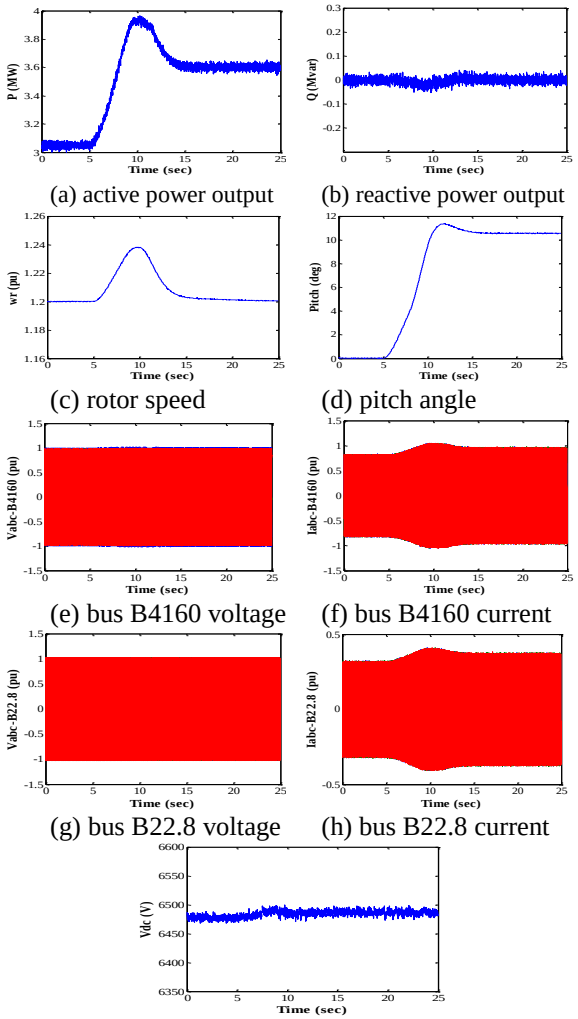

(a) active power output (b) reactive power output

(c) rotor speed (d) pitch angle

(e) bus B4160 voltage (f) bus B4160 current

(g) bus B22.8 voltage (h) bus B22.8 current

(i) dc-link voltage

Fig. 10 Dynamic responses of the DFIG under the gradation wind action

4.3 Dynamic simulation of the DFIG under a random wind action

The speed variation of the random wind studies here is shown in Fig. 8, which randomly varies between 12.3m/s to 17.6m/s. The variations of active power, rotor speed, and pitch angle vary with the wind speed change are shown in Fig. 11(a), 11(c), and 11(d), respectively. The voltages at bus B4160 and B22.8 shown in Fig. 11(e) and 11(g) maintain at 1pu. The currents at bus B4160 and B22.8 shown in Fig. 11(f) and 11(h) vary with the wind speed fluctuation. The DC link voltage varies with the wind speed fluctuation much obviously under the random wind action as shown in Fig. 11(i).

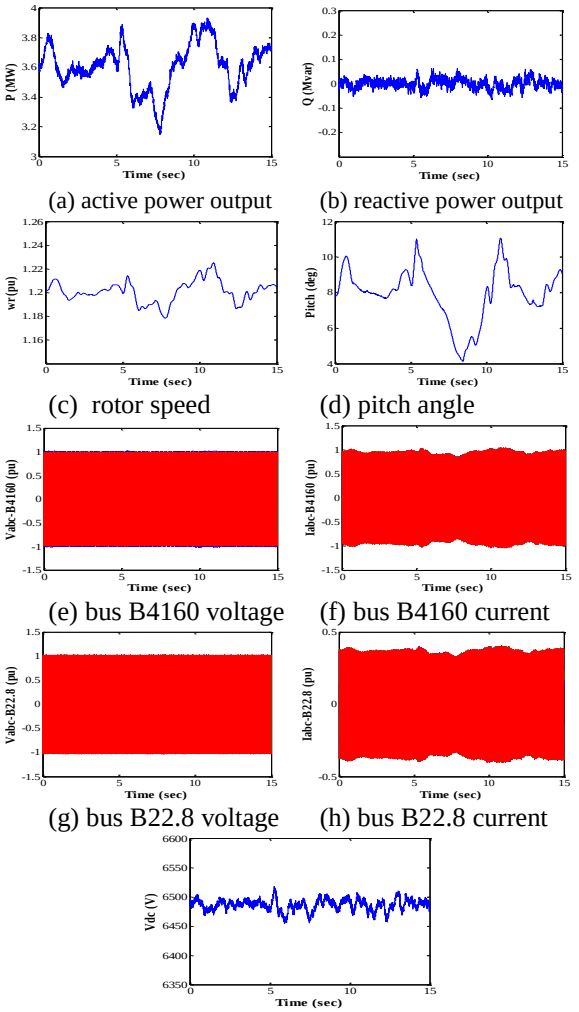

(a) active power output (b) reactive power output

(c) rotor speed (d) pitch angle

(e) bus B4160 voltage (f) bus B4160 current

(g) bus B22.8 voltage (h) bus B22.8 current

(i) dc-link voltage

Fig. 11 Dynamic responses of the DFIG under the random wind action

5. Conclusion

This paper studies the effect of wind speed fluctuation on the doubly fed induction generator connected to power system. The mathematical models of a 3.6MW doubly fed induction generator and different wind patterns are derived. The

MATLAB/Simulink software is then used to model the wind, wind turbine, doubly fed induction generator, and its controllers. Simulation results obtained from the model are used to analyze the effects of different wind speed fluctuation on system dynamic responses, which could be a useful reference for initial scheme of a 3.6MW DFIG connected to power systems.

References

[1] W.J. Zeng, "Blow a New Opportunity for Energy-On the Wind Power and Renewable Energy," *The Monthly Publication of Taiwan Power*, Vol. 516, 2004, pp. 4-11.

[2] S. Muller, M. Deicke, W. Rik, and De Doncher, "Doubly Fed Induction Generator System for Wind Turbines," *IEEE Industry Application Magazine*, Vol. 8, No. 3, May 2002, pp. 26-32.

[3] R. Pena, J. Clare, and G. Asher, "Doubly Fed Induction Generator Using Back-to-Back PWM Converters and Its Application to Variable-Speed Wind Energy Generation," *IEE Proceedings, Electric Power Applications*, Vol. 143, No. 3, May 1996, pp. 231-241.

[4] S. Muller et al., "Adjustable Speed Generator for Turbines Based on Doubly-Fed Induction Machines and 4 Quadrant IGBT Converter Linked to the Rotor," *Proceedings of IEEE Industry Applications Conference*, Vol. 4, Oct. 2000, pp. 2249-2254.

[5] Lie Xu, Yi Wang, "Dynamic Modeling and Control of DFIG-Based Wind Turbines Under Unbalanced Network Conditions," *IEEE Transactions on Power Systems*, Vol. **22,** Feb. 2007, pp. 314–323.

[6] A. Tapia, G. Tapia, J.X. Ostoiaza and J.R. Saenz, "Modeling and control of a wind turbine driven doubly fed induction generator," *IEEE Transactions on Energy Conversion*, Vol. 18, 2003, pp. 194-204.

[7] L. Mihet-Popa, F. Blaabjerg, and I. Boldea, "Wind Turbine Generator Modeling and Simulation Where Rotational Speed Is the Controlled Variable," *IEEE Transactions on Industry Applications*, Vol. 40, No.1 , 2004, pp. 3-10.

[8] H.C. Chen, J.C. Qiu, and L.Y. Jhang, "The Influence Analysis of Wind-Speed Fluctuation on the Dynamic of a Wind-Diesel Hybrid Power System," *The 1th Intelligent Living Technology Conference, National Chin-Yi Institute of Technology,* 2006, pp. 2041-2048.